engineering proceedings

MDPI

Proceeding Paper

Fatigue Analysis of Draw Gears in Freight Trains †

Edoardo Risaliti [1,*], Francesco Del Pero [1], Alessandro Giorgetti [2], Luciano Cantone [3] and Gabriele Arcidiacono [1]

[1] Department of Engineering Science, Guglielmo Marconi University, 00193 Rome, Italy; f.delpero@unimarconi.it (F.D.P.); g.arcidiacono@unimarconi.it (G.A.)
[2] Department of Industrial, Electronic and Mechanical Engineering, Roma Tre University, 00146 Rome, Italy; alessandro.giorgetti@uniroma3.it
[3] Department of Enterprise Engineering, Tor Vergata University, 00133 Rome, Italy; luciano.cantone@uniroma2.it
* Correspondence: e.risaliti@unimarconi.it
† Presented at the 53rd Conference of the Italian Scientific Society of Mechanical Engineering Design (AIAS 2024), Naples, Italy, 4–7 September 2024.

Abstract: The majority of freight trains are characterized by a braking system that does not guarantee synchronous braking between different wagons. This results in the generation of considerable in-train forces during emergency braking operations, which are sometimes imposed by the railway infrastructure due to certain running speeds being exceeded. The magnitude of in-train forces is contingent upon a number of factors, the most significant ones being the length, mass and load composition of the trainset, in addition to the specific braking imposed. The application of excessive compressive in-train forces has the potential to cause the wagon to derail, particularly if the wagon is lightweight and traversing a small radius curve. Similarly, excessive tensile in-train forces applied to the screw couplers can cause them to fail, typically through fatigue, resulting in train disruption and necessitating the recovery of both portions of the trainset. The objective of this study is to perform a preliminary analysis of the UIC (International Union of Railways) unified screw couplers fatigue phenomenon, employing load spectra computed by the UIC 1.4.6 software *TrainDy*. A possible future development is developing a maintenance model functional to predict the extent of damage in freight wagon screw couplers during their service life.

Keywords: screw couplers; freight trains; fatigue; finite element model

Academic Editors: Umberto Galietti, Enrico Armentani, Davide Castagnetti, Vigilio Fontanari, Aurelio Somà and Nicola Bonora

Published: 27 February 2025

Citation: Risaliti, E.; Del Pero, F.; Giorgetti, A.; Cantone, L.; Arcidiacono, G. Fatigue Analysis of Draw Gears in Freight Trains. *Eng. Proc.* **2025**, *85*, 46. https://doi.org/10.3390/engproc2025085046

1. Introduction

Longitudinal Train Dynamics (LTD) is defined as the relative motion between wagons in their movement along the traveling direction. This movement is caused by the elasticity of the connecting elements between wagons. Such a phenomenon occurs during both acceleration and braking phases, and it is influenced by a number of factors, including the train length and mass, the type of wagons (and their respective braking characteristics) and the speed and elevation of the track [1,2]. In particular, the braking phase is of great importance for the longitudinal train dynamics, as the unified brake, which is used in freight trains in the major European countries, does not guarantee the application of braking action in a synchronous manner between the different wagons [3]. The asynchronous braking action among wagons results in a delay in the application of the brakes, particularly in long trains. In such a scenario, also depending on the brake position, the first wagons brake immediately, while the subsequent wagons brake with a delay, contingent upon the emptying of the brake pipe. This inevitably leads to the generation of high values of

longitudinal compressive forces, given that the first wagons brake while the last wagons do not.

To effectively address the consequences of non-synchronous braking, it is fundamental to not only regulate the mass and length of trains but also to monitor the braking position [4,5]. In accordance with IRS 40421, a freight train must comply with a series of criteria to operate on the international rail network, including requirements for length and mass. These limits are based on operational practice within the member countries of the Union Internationale des Chemins de fer (UIC) and exceptions are granted on the basis of bilateral agreements. Furthermore, additional limits may be applied if it is demonstrated that the probability of derailment caused by excessive longitudinal compressive forces (or in-train) at the buffers is less than that of the trains permitted to run [6].

While longitudinal compressive forces are the most critical of the longitudinal forces (as they can cause train derailment), the consequences of excessive tensile forces on the connecting elements between wagons should not be overlooked. Such forces can lead to the "disruption" of the train and the consequent interruption of service, with repercussions on the movement of other trains on the same line. The wagons are maintained in a relatively controlled position by the buffers (which prevent an excessive approach), and by the coupling elements (which prevent an excessive spacing). With regard to the latter, each wagon is equipped with a draw gear at both ends, comprising a hook and a screw coupler. An example of the assembly is shown in Figure 1 [7].

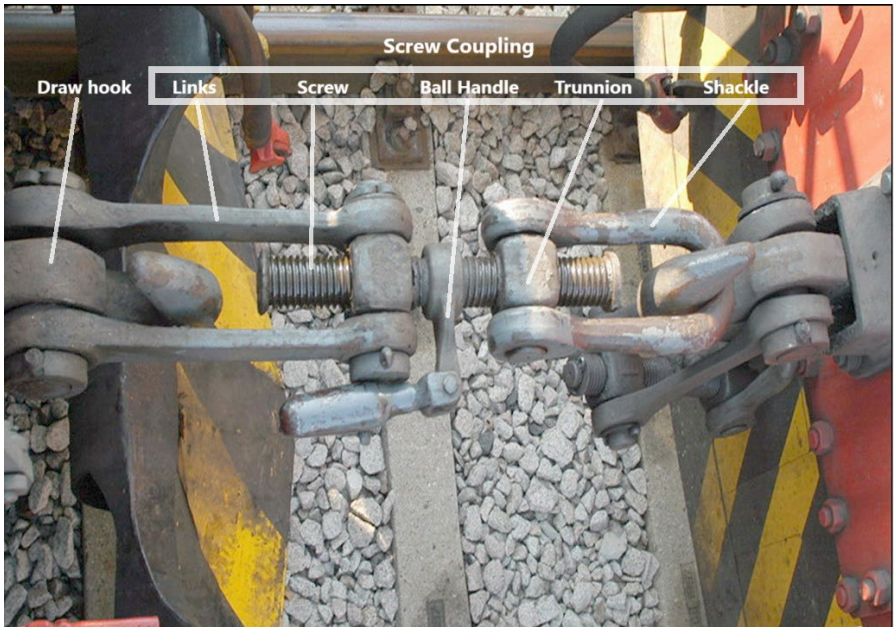

Figure 1. Example of the connection assembly between the wagons considered in the case study [7].

The screw is considered to be the weakest component, susceptible to failure under excessive longitudinal tensile forces. According to UIC EN 15566 [8], draw gear and screw coupling are classified into three categories based on their maximum tensile force: 1 MN, 1.2 MN, 1.5 MN. For the 1 MN screw coupling, the minimum breaking lod is 850 kN, while the maximum is 980 kN. In comparison, the draw gear and draw hook have a minimum breaking load of 1 MN. Indeed, it is typical that the screw coupling breaks at the screw. However, there are also cases in which failure occurs at the coupling links or even at the draw hook. In ordinary operation, the screw coupling is subjected to tensile forces during acceleration and braking phases due to longitudinal dynamics. From a mechanical perspective, it is susceptible to fatigue cycles that can lead to its deterioration. However,

failure can also occur in a static manner due to the presence of excessive tensile forces resulting from braking after acceleration [9].

In light of a review of the literature on the structural integrity criticalities of freight train screw couplings, this study performs a preliminary fatigue analysis of the screw (prEN 15566:2018) based on load spectra computed by the UIC software TrainDy [10], based on version 1.4.6: this software has been initially developed by the University of Rome Tor Vergata, with the financial and technical support of Faiveley Transport (a company of Wabtec group), and since 2007 it is owned by the UIC; the software is currently developed by the TrainDy Special Group within the UIC. The main target of the work is to evaluate the extent of possible fatigue at different points of the screw to forecast the extent of damage incurred by such a component over its operational lifespan.

2. Materials and Methods

A simulation was conducted using the finite element method (FEM) with the Altair HyperWorks software 2024.1 [11]. The screw geometry was obtained from the norm [9]. The screw was 445 mm in length, with a diameter of 52 mm in the central area and an average diameter of 46.85 mm at the thread location. The areas deemed critical for analysis were those situated between the central zone and the thread, since they exhibited the lowest resistance, with a diameter of 42.5 mm. Using CAD software (SolidEdge 2023) [12], an initial static analysis of the component was conducted.

The FE model (Figure 2) consists of about 2.1 million 3D elements (tetrahedral CTETRA4 and pyramidal CPRYA). The density of the mesh was 1 mm both in the areas where loads/constraints are applied, and in the central zone area where the resistant section is smaller (see boxes a, b and c in Figure 2). In the other zones, we decided to increase the mesh size from 2 up to 4 mm to decrease the computational costs. The fixed support and the application of loads were modeled as shown: using 10 groups of RBE3 elements which were connected to the central node on the mean circumference of the screw (Figure 3).

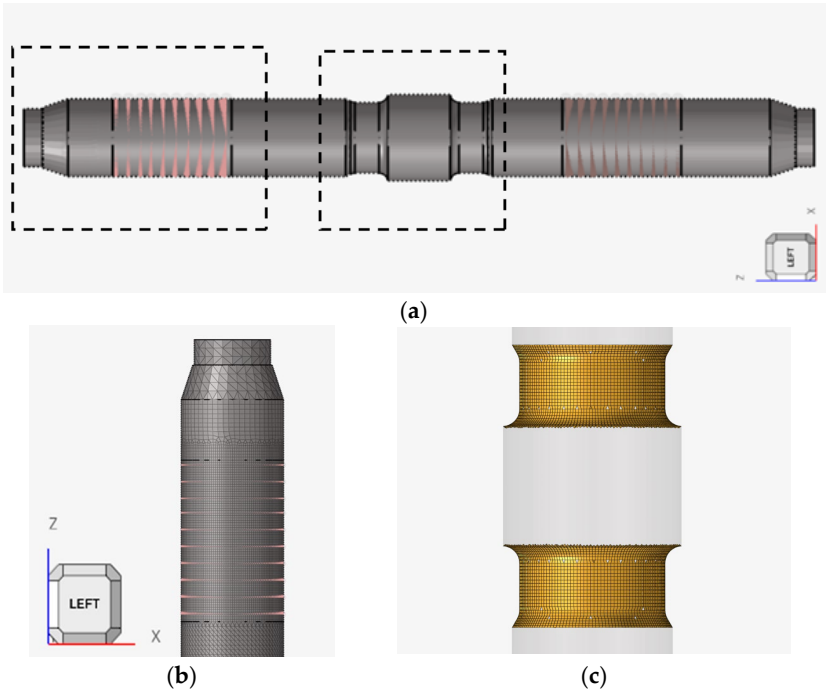

Figure 2. (**a**) FE model of the complete screw, with the application points of the RBE3 elements in light pink and dark pink; (**b**) enlargement of the left window: detail of the FE modeling in the

connection area between the screw and the mother screw with visualization; (**c**) enlargement of the middle window: detail of the FE modeling in the middle area.

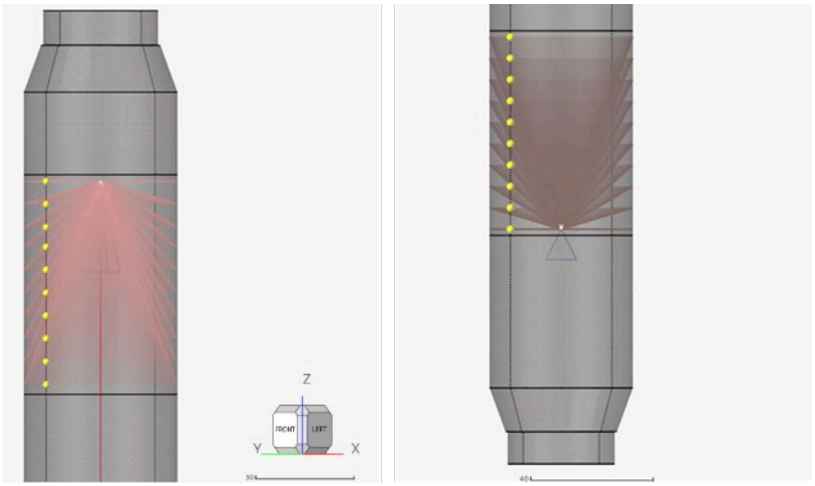

(**a**) (**b**)

Figure 3. Detail of the FE model of the RBE3 elements. (**a**) Point of load application; (**b**) point of application of the interlocking constraint.

The selected nodes along the circumference were spaced 7 mm apart (thus, there were seven elements) to model the pitch of the screw and the screw–mother contacts. Ten groups of RBE3 elements were chosen since the length of the connection via the mother screw turned out to be 75 mm long. Such a model configuration the stress pattern on each screw thread to be simulated quite well from a qualitative point of view. On the contrary, this method is not effective for simulating load distributions at a quantitative level. This is because RBE3 elements do not allow local deformations to be captured; in addition, distributing the load node by node may result in higher stresses being encountered. That said, these considerations are of secondary importance, as the objective of the work is investigating the behavior of the central regions of the tie rod, without focusing on connections.

A second static simulation was performed using the model shown in Figure 4.

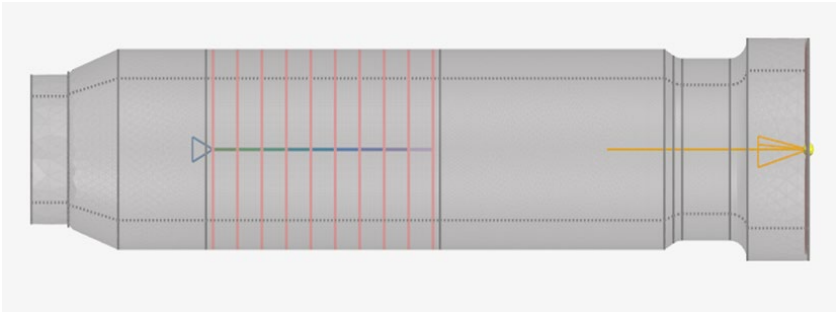

Figure 4. Modeling of the component split in half. Left is the modeling of the screw–mother screw connection with the differently elastic constant (differently colored) CBUSH elements connected to the constrained node. The triangle is the constraint application. On the right is the application of the load (yellow indicator), distributed via RBE3 elements over the entire sectioned surface.

In this case, the model was split in half, thus reducing the number of TETRA4 elements to 850,000 (only TETRA4 elements are used). The forces were applied in a distributed manner over the entire cut surface of the screw, while for the interlocking constraint and the associated screw–mother screw connection, a different configuration was adopted with respect to the previous version of the model (Figure 5).

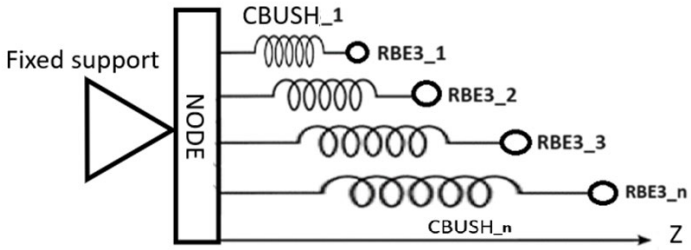

Figure 5. Schematic diagram of the simulation of the screw-to-screw connection using CBUSH elements.

Adopting a simplified version of the Masing model [13], 10 CBUSH elements are connected to the constrained nodes. Each CBUSH element is characterized by an elastic stiffness given by the following formula:

$$k_n = \frac{EA}{nl}$$

where k is the elastic constant, E is the Young's modulus, A is the resistant section, n is the elastic element considered and l is the screw pitch. For the resistant section, the average screw diameter was chosen.

The RBE3 elements were 7 mm apart to account for the screw pitch. The first CBUSH element was the most rigid, and subsequent elements were gradually less rigid. Such an approach better captures the load distribution between threads, as provided in Reference [14].

However, again this modeling turns out to be too simplistic to model the connection, since it is well known that stress concentrations are influenced by the thread profile shape, the radius at the root and the contact conditions [15,16]. Using CBUSH elements to represent each thread and measuring load at the nodes of the mean circumference means that information about the local stress variations occurring at the roots of the threads is lost [17,18]. That said, the main target of the model was not to perform a local analysis of the connection between the screw and the hook, but an analysis of the areas with the smallest resistant cross-section. Additionally, such a modeling approach was chosen to have a distribution of load lines from the connection to the central zone of the screw, with the latter being the most representative.

After performing static simulations, the HyperLife software 2024.1 was used [19] to perform fatigue analyses starting with the data from the FEM simulations. HyperLife uses Palmgrem–Miner's cumulative damage method [20,21] to calculate the service life of a component under varying loads; such a method shows that each repeated load cycle contributes partially to the overall damage of the component. The version of the software used does not consider the effects of surface roughness that could affect the fatigue life of the component.

As shown in Figure 6, we decided to implement a uniaxial analysis through S-N curves and to use Goodman's method to correct the sensitivity factor according to the mean stress [22].

As shown in Figure 6, the material selected for analysis was a 4140 Steel that was quenched and tempered, which appears to be consistent with the standard for the design of the component. The analysis is focused on two train operations, taken from load spectra computed by the UIC 1.4.6 software *TrainDy* [10]. The first one is defined as "Emergency Braking" (EB), and it shows a trainset traveling at a speed of 30 km/h performing emergency braking. The second one is referred to as the "Traction Emergency Brake" (TEB), and it shows that the trainset is at a standstill, after which it accelerates and then brakes

abruptly by emergency braking. The computation of in-train forces was performed using the TrainDy software, as suggested by the IRS 40421.

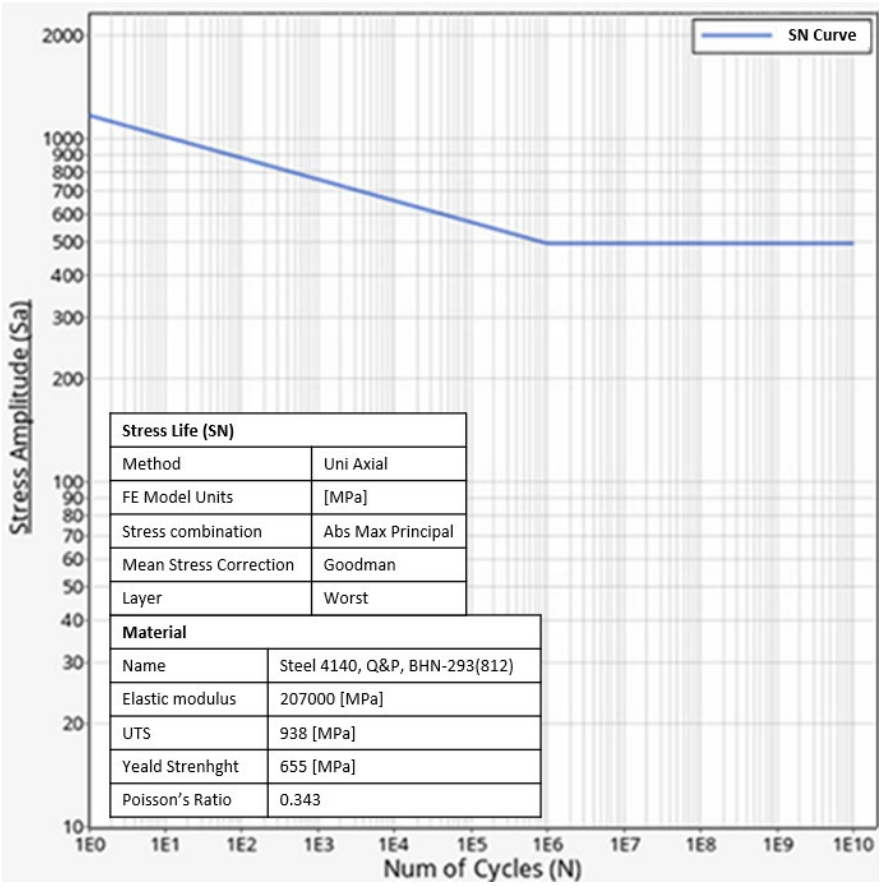

Figure 6. Setting details for using Hyerlife: top left shows the mechanical properties of AISI4140 steel and the right shows an S-N diagram of the same material with stress amplitude in MPa as the ordinate. Bottom left shows the settings for the S-N analysis.

Figure 7 depicts the trends in the stresses acting on each screw coupling of the convoy during the emergency braking (referred to as the "block"). The ordinate provides the intensity of the load (in kN), while the abscissa provides elapsed time (in s).

Image "a" refers to the TEB event, while image "b" refers to the EB event. The two events were employed to quantify the extent of damage that occurred in the screw coupling by applying the following four limit cases:

1. TEB event considering block 1 (maximum tension in the first phase);
2. TEB event considering block 22 (maximum tension in the second phase);
3. EB event considering block 1 (maximum tension in the first phase);
4. EB event considering block 13 (maximum tension in the second phase).

According to the above approach, we decided to consider only the TEB event, given that the EB event failed to prove critical for the component, as shown in Figure 8 and critically discussed in the Section 3. Consequently, for the second analysis, the following blocks were considered:

1. TEB event considering block 1 (maximum tension in the first phase);
2. TEB event considering block 23 (maximum tension in the second phase).

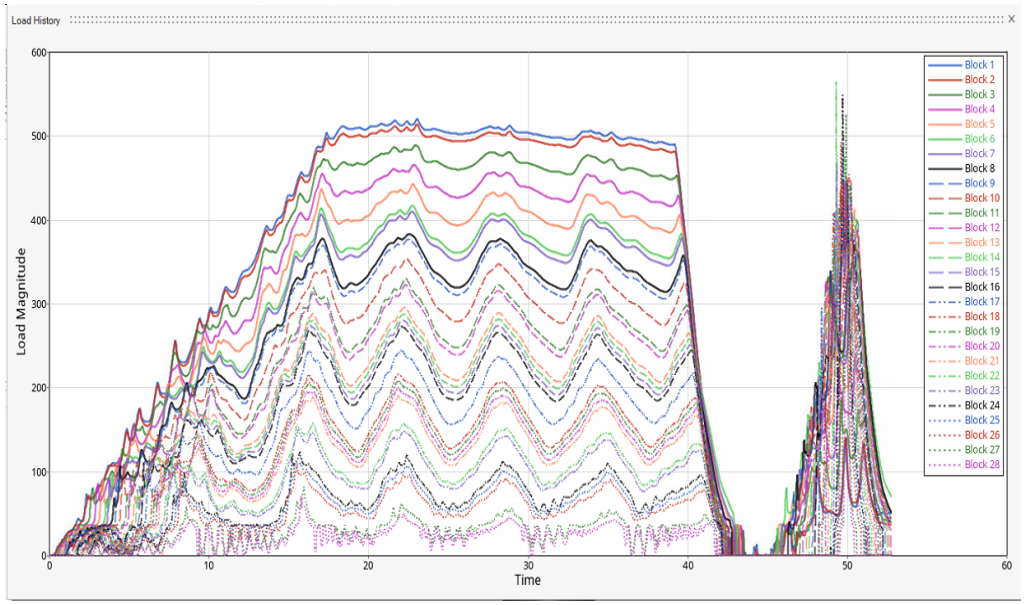

(**a**)

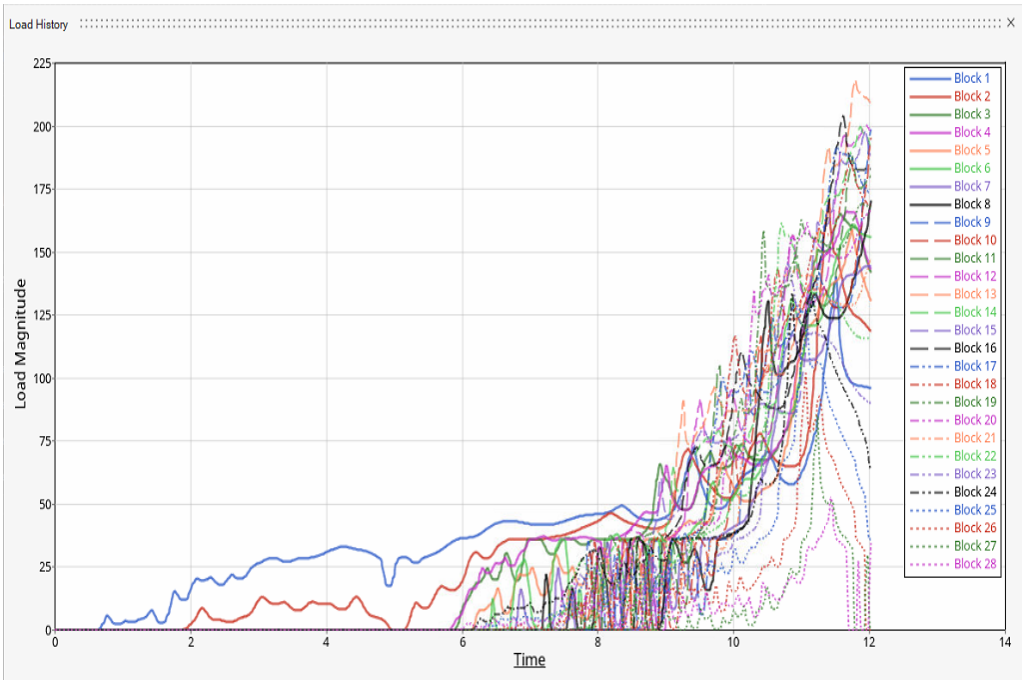

(**b**)

Figure 7. Load history for each screw coupling in the simulated train. Each block corresponds to a screw coupling: (**a**) trend in loads with TEB operation; (**b**) trend in loads with EB operation.

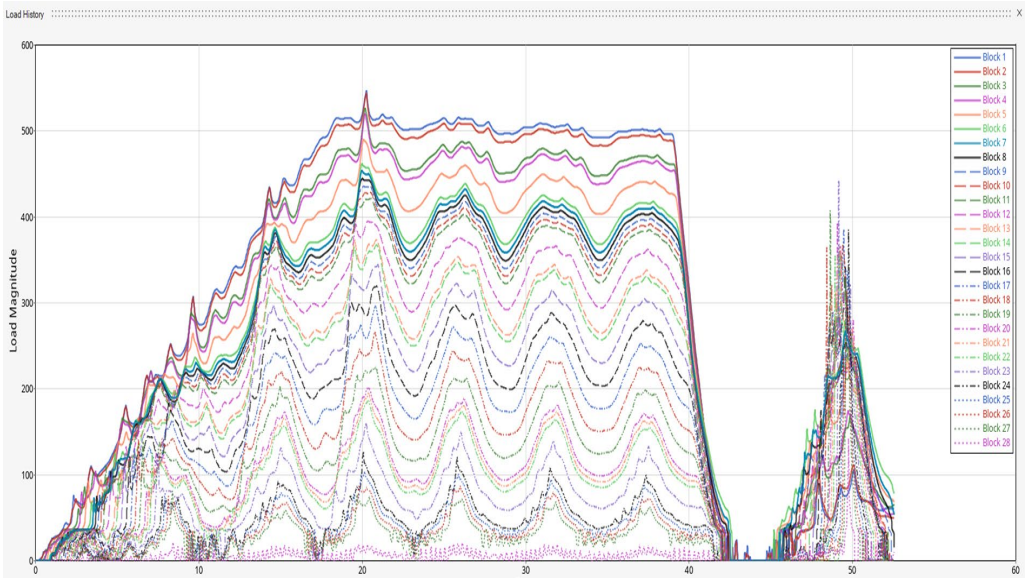

Figure 8. Trend in loads with TEB operation for the second FE model.

3. Results and Discussion

This section provides the results of both the static and fatigue simulations for the two models described above. Table 1 shows the list of analyses performed.

Table 1. List of analyses performed and shown in the results.

Code	Type Analysis	Operation	Reference Figure Operation	Block	FE Model
A1	Static	TEB (Max Load)	7a	22	Full
A2	Fatigue	TEB	7a	1	Full
A3	Fatigue	TEB	7a	22	Full
A4	Fatigue	EB	7b	1	Full
A5	Fatigue	EB	7b	13	Full
A6	Static	TEB (Max Load)	8	1	Half
A7	Fatigue	TEB	8	1	Half
A8	Fatigue	TEB	8	23	Half

The results of A1 obtained through the first model described above are shown in Figure 9.

The Figure shows that the screw has a deformation along the z-axis with a displacement of about 0.34 mm. The screw is subjected to the maximum tensile force, recorded in block 22 in Figure 7, which is 575 kN. The central zone of the screw (characterized by the least resistant section of the component) does not reach the yield strength value; indeed, a stress between 325 and 650 MPa was measured, against a yield strength of 655 MPa.

On the other hand, the RBE3 elements qualitatively represent the first thread, as the most loaded, and the subsequent threads, as less loaded, well.

Figure 10 shows the results of A2 and A3, the fatigue analyzes of the TEB event. In particular, we wanted to analyse how much the emergency braking affects the fatigue life of the analysed component.

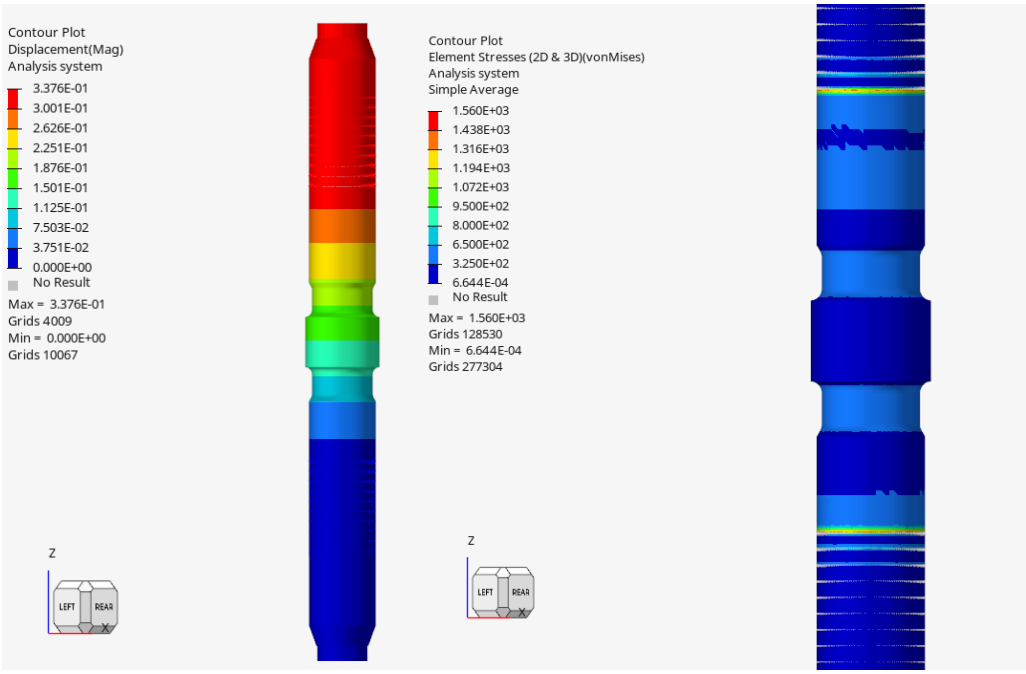

(**a**) (**b**)

Figure 9. FEM analysis of the screw. (**a**) Displacement results; (**b**) element stresses results.

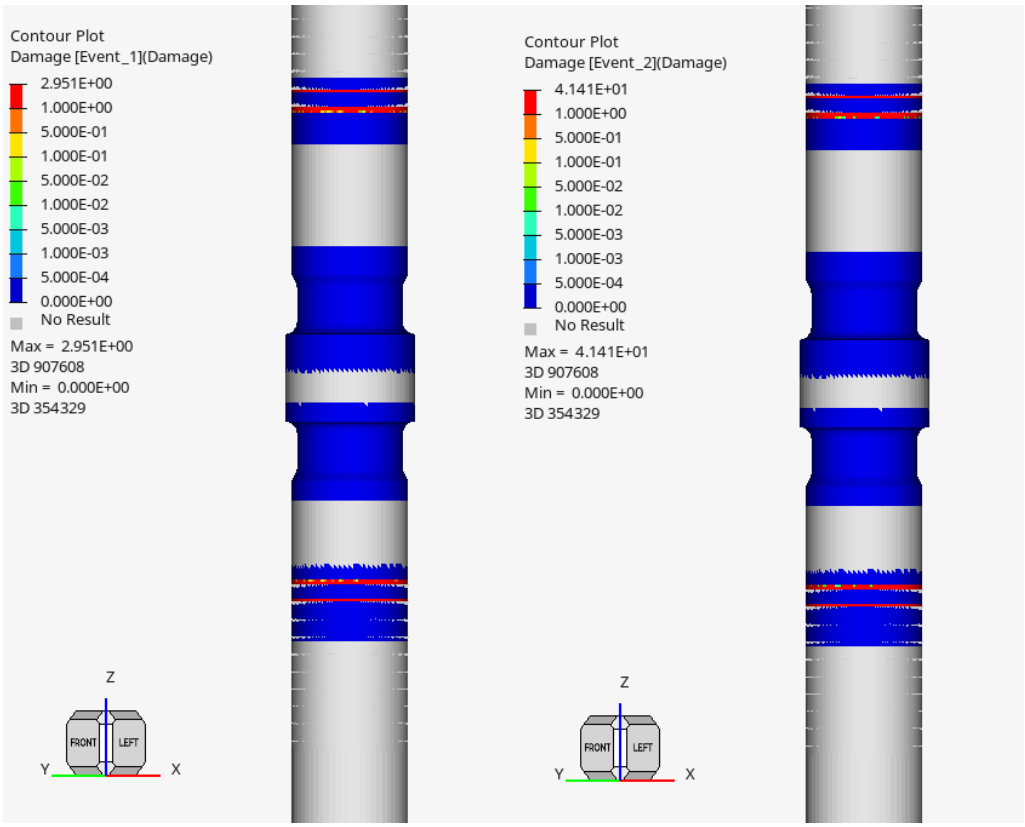

(**a**) (**b**)

Figure 10. Fatigue analysis of the screw with TEB operation. (**a**) A2 results; (**b**) A3 results.

For both event 1 (corresponding to block 1) and event 2 (corresponding to block 23), the fatigue life of the screw in the central zone is not significantly reduced, since the damage index is close to zero. Values higher than 1 (indicating component failure) are found in areas where constraints and loads are applied, which, as mentioned above, are not significant from a physical point of view.

Figure 11 shows the analysis of the simulations for the EB operation (A4 and A5).

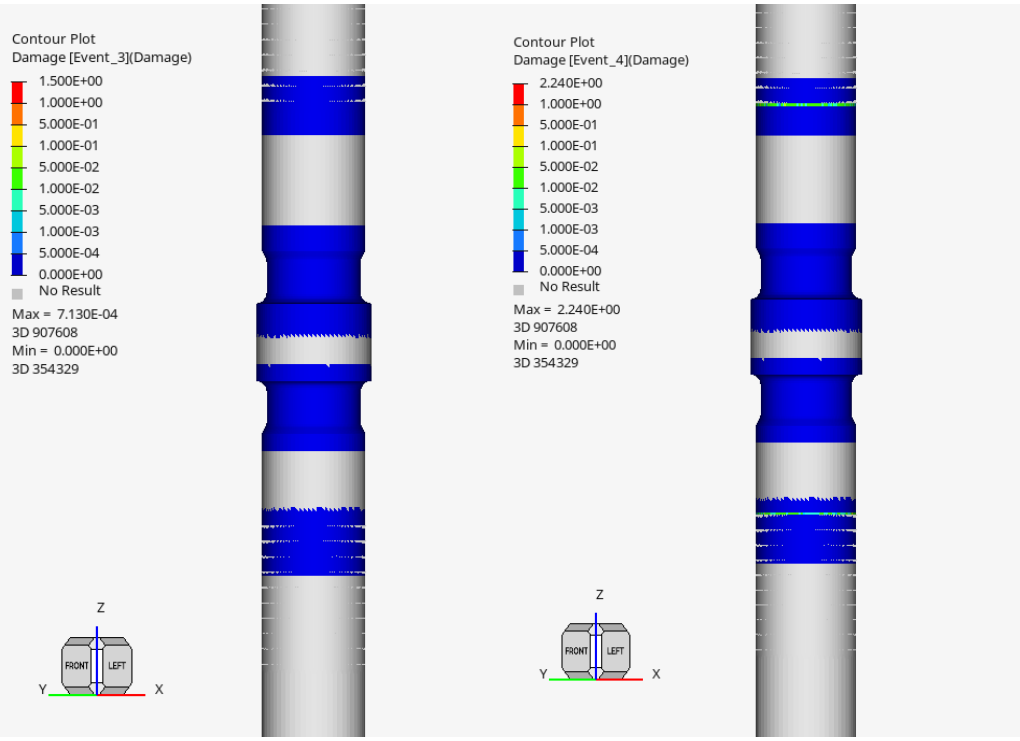

(**a**) (**b**)

Figure 11. Fatigue analysis of the screw with EB operation. (**a**) A4 results; (**b**) A5 results.

In both cases (block 1 and block 13), there is no reduction in fatigue life due to the load cycle. In particular, there is no damage in the connector caused by loads of block 1; on the other hand, minor damage is observed in the thread areas due to block 13 load cycles. In view of these results, it is concluded that the EB event is not particularly severe for the component analysed. For this reason, in the second FE modeling (modeling of half the component), we decided to simulate only the TEB event; A6's results are reported in Figure 12.

As shown in the Figure, the static analysis (using an equivalent load of 570 kN in the -Z direction) shows a deformation of 0.20 mm; this result is consistent with previous studies, because the component is globally stiffer than in previous simulations due to its reduced length. Figure 12 also shows that in the area with the smallest resistant section the maximum equivalent stress is between 500 and 650 MPa, which is lower than the yield strength of the considered material. Stress peaks were detected in areas where constraints were applied, with the reason for this being the same as the one explained for dealing with the first version of the model.

Figure 13 shows A7 and A8's results.

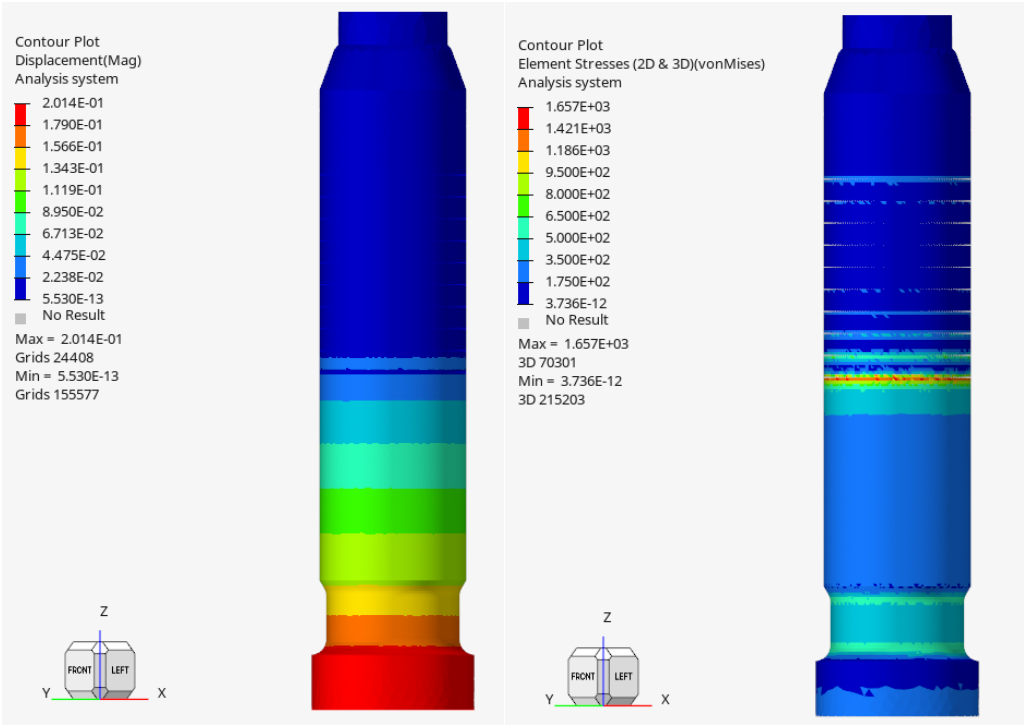

(**a**) (**b**)

Figure 12. A6 FE model analysis of the half screw. (**a**) Displacement results; (**b**) element stresses results.

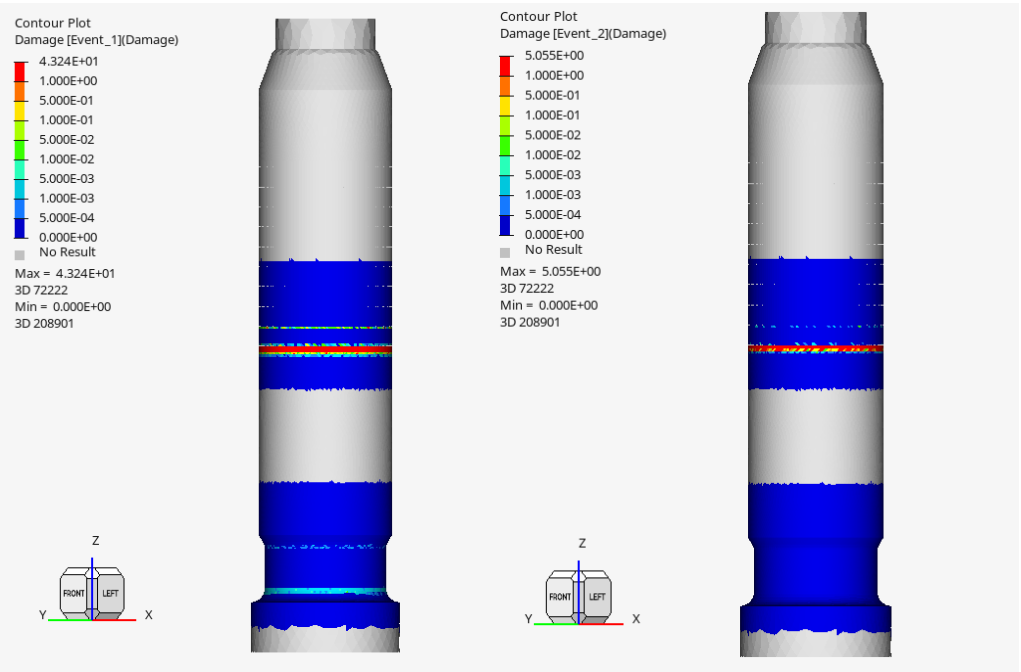

(**a**) (**b**)

Figure 13. Fatigue analysis of the half screw with TEB operation. (**a**) A7 results; (**b**) A8 results.

For block 1 (event 1), the damage is in the range between 1×10^{-3} and 5×10^{-3} of the area of minimum resistant section. Considering the inverse of the damage as an estimate of the number of cycles, the component could withstand approximately 200 cycles subjected to load cycles of TEB block 1. In other words, this component will be able to resist these emergency braking operations approximately 200 times.

On the other hand, no damage is recorded in the central zone for block 23 (event 2).

In this context, with the analyses performed, this component would appear to withstand such emergency cycles, without them significantly affecting the component's fatigue life.

4. Conclusions

The article provides a preliminary analysis of the fatigue phenomenon on a UIC unified coupling device. The "Traction Emergency Braking" and "Emergency Braking" load simulations were computed by TrainDy v1.4.6 and used to see whether and how much they affect the operational life of the component by causing fatigue damage. We performed static and fatigue analyses of the railway screw coupling using the finite element method (FEM) using the Altair HyperWorks software 2024.1. Two versions of the FE model were developed. The first one considers the entire screw and uses RBE3 elements to model the constraints; the second one considers only half of the screw and uses CBUSH elements to account for the stiffness of the screw-to-screw connection. Both versions of the model were statically simulated to provide a baseline for fatigue analysis, which was conducted using the HyperLife software 2024.1. The static analysis of the components considers a tensile force of 570 kN along the z-axis, which turns out to be the maximum tensile force that occurs in the events considered. For both FEM simulations, no equivalent stress values were recorded that would cause the screw to yield. The results of the fatigue investigation show that the considered load cycles do not affect the component's duration, except in the case of TEB block 1 modeled in the half-component simulation, which provides a rate of damage between 1×10^{-3} and 5×10^{-3}. Possible future developments of the study include the use of fatigue results for conceiving a predictive maintenance model that is able to forecast the extent of damage in the turn buckle during its operational lifetime.

Author Contributions: Conceptualization, G.A., A.G. and L.C.; methodology, L.C., E.R., F.D.P. and A.G.; software, E.R. and L.C.; validation, L.C. and A.G.; formal analysis, E.R.; investigation, E.R. and F.D.P.; resources, G.A.; data curation, E.R. and L.C.; writing—original draft preparation, E.R. and F.D.P.; writing—review and editing, E.R., F.D.P., A.G., L.C. and, G.A.; visualization, E.R. and F.D.P.; supervision, G.A.; project administration, L.C. and G.A.; All authors have read and agreed to the published version of the manuscript.

Funding: This research received no external funding.

Institutional Review Board Statement: Not applicable.

Informed Consent Statement: Not applicable.

Data Availability Statement: The raw data supporting the conclusions of this article will be made available by the authors on request.

Conflicts of Interest: The authors declare no conflict of interest.

References

1. Cantone, L. TrainDy: The new Union Internationale des Chemins de Fer software for freight train interoperability. *Proc. Inst. Mech. Eng. Part F J. Rail Rapid Transit* **2011**, *225*, 57–70. [CrossRef]
2. Arcidiacono, G.; Berni, R.; Cantone, L.; Nikiforova, N.D.; Placidoli, P. Fast Method to Evaluate Payload Effect on In-Train Forces of Freight Trains. *Open Transp. J.* **2018**, *12*, 77–87. [CrossRef]
3. Wu, Q.; Cole, C.; Spiryagin, M.; Chang, C.; Wei, W.; Ursulyak, L.; Shvets, A.; Murtaza, M.A.; Mirza, I.M.; Zhelieznov, K.; et al. Freight train air brake models. *Int. J. Rail Transp.* **2023**, *11*, 1–49. [CrossRef]
4. Cantone, L.; Arcidiacono, G. A study on releasing manoeuvre to improve freight safety and efficiency. *Int. J. Mech. Eng. Technol.* **2018**, *9*, 899–909.
5. Cantone, L.; Arcidiacono, G.; Placidoli, P. Autonomous Determination of Pneumatic Parameters of Traindy. *Int. J. Mech. Eng. Technol.* **2018**, *9*, 1507–1515.

6. Popović, M.V.; Momčilović, D.; Tanasković, J.; Sedmak, A. Testing of the condition and performance of coupling links from screw couplings of train. *Eng. Fail. Anal.* **2024**, *161*, 108331.
7. Ferrovie Nord. ISTRUZIONE PER IL SERVIZIO DEI MANOVRATORI in uso sull'infrastruttura ferroviaria gestita da FERROVIENORD. 2019. Available online: https://www.ferrovienord.it/wp-content/uploads/2022/01/ISM_Edizione_2019.pdf (accessed on 17 February 2025).
8. Popović, M.V.; Tanasković, J.; Međedović, N. Review of failure analysis of coupling systems on trains. *Procedia Struct. Integr.* **2023**, *48*, 252–259. [CrossRef]
9. EN 15566:2022 Railway Applications—Railway Rolling Stock—Draw Gear and Screw Coupling. Available online: https://www.din.de/en/getting-involved/standards-committees/fsf/publications/wdc-beuth:din21:345557818 (accessed on 17 February 2025).
10. TrainDy Website. Available online: https://uic.org/special-groups/traindy/ (accessed on 6 July 2024).
11. Altair Website. Available online: https://altair.com/ (accessed on 1 July 2024).
12. Siemens Website. Available online: https://solidedge.siemens.com/it/free-software/overview/ (accessed on 6 July 2024).
13. Beck, J.L.; Pei, J.S. Demonstrating the power of extended Masing models for hysteresis through model equivalencies and numerical investigation. *Nonlinear Dyn.* **2022**, *108*, 827–856. [CrossRef]
14. Liu, J.; Ouyang, H.; Ma, L.; Zhang, C.; Zhu, M. Numerical and theoretical studies of bolted joints under harmonic shear displacement. *Lat. Am. J. Solids Struct.* **2015**, *12*, 115–132.
15. Bickford, J. *An Introduction to the Design and Behavior of Bolted Joints, Revised and Expanded*; Routledge: London, UK, 2018.
16. Giannella, V.; Romano, D.; Greco, M.; Molitierno, R.; Sepe, R.; Armentani, E. Wired threaded inserts in joints with steel screws and aluminium nuts: A parametric study on their effectiveness. *Forces Mech.* **2024**, *14*, 100258. [CrossRef]
17. Kenny, B.; Patterson, E.A. Load and stress distribution in screw threads. *Exp. Mech.* **1985**, *25*, 208–213. [CrossRef]
18. Zhao, H. Stress concentration factors within bolt-nut connectors under elasto-plastic deformation. *Int. J. Fatigue* **1998**, *20*, 651–659.
19. Hyperlife Website. Available online: https://altair.com/hyperlife (accessed on 1 July 2024).
20. Miner, M.A. Cumulative damage in fatigue. *J. Appl. Mech.* **1945**, *12*, 159–164.
21. Palmgren, A. Die Lebensdauer Von Kugellagern. *VDI-Z.* **1924**, *68*, 339–341.
22. Zhang, Z.; He, Z.; Yang, B.; Wang, Y.; Xiao, S.; Hou, M.; Guo, T. An improved Goodman-Smith fatigue limit diagram for railway vehicle base metals and welded structures. *Int. J. Fatigue* **2024**, *182*, 108160. [CrossRef]